describes the relativistic effect and nuclear polarizability. (Similar calculations for ^{14}N, ^{15}N, and ^{12}C agree within 0.1% with this ^{16}O calculation.) In this figure the data for a given beam energy and projectile have been averaged over the measured backward scattering angles (θ_{lab} = 140°, 145°, 150°, etc.) in order to improve the statistics. It can be seen in Fig. 3 that above 20 fm^{-1} (which corresponds roughly to E_{lab} = 20 MeV for ^{16}O) the data agree substantially with the prediction, but below 20 fm^{-1} the data lie slightly above the prediction. This enhancement below 20 fm^{-1} may in part be caused by our neglect of atomic polarizability. It should be pointed out that the screening effect we are subtracting from the data to make this plot changes by more than 0.8% from 10 to 20 MeV; thus a 10% underestimation of this screening effect could give rise to the discrepancy.

In summary we have seen unambiguous evidence for the presence of a combination of nuclear polarizability and the relativistic effect. It is not possible from numerically fitting the data *alone* to determine the relative importance of these two effects. Nevertheless, if one sets nuclear polarizability at its normal value with a 25% error one has a measurement of relativistic dynamics with 30% accuracy. By taking the opposite tack and assuming the validity of relativistic dynamics, one has a measurement of averaged nuclear polarizability with 25% accuracy. Static electron screening appears to be reasonably accurate (to within 10%) while the measurement of vacuum polarization was masked by the uncertainties in atomic screening.

This work was supported in part by the U. S. Department of Energy.

[a]Present address: NSCL, Michigan State University, East Lansing, Mich. 48824.
[b]Present address: Nuclear Physics Laboratory, University of Colorado, Boulder, Colo. 80309.
[c]Present address: Westinghouse, Hanford, Wash.

[1]K. Alder and A. Winther, *Electromagnetic Excitation* (North-Holland, Amsterdam, 1975).
[2]J. Rasmussen *et al.*, Nucl. Phys. A341, 149 (1980).
[3]W. Schäfer *et al.*, Nucl. Phys. A272, 493 (1976).
[4]K. C. Wang *et al.*, Phys. Lett. 79B, 170 (1978).
[5]T. E. O. Ericson and J. Hüfner, Nucl. Phys. B47, 205 (1972).
[6]G. Baur *et al.*, Nucl. Phys. A288, 113 (1977).
[7]J. Ahrens *et al.*, Nucl. Phys. A251, 479 (1975).
[8]E. G. Fuller and Evans Hayward, in *Nuclear Reactions*, edited by P. M. Endt and P. B. Smith (North-Holland, Amsterdam, 1962), Vol. II, p. 113.
[9]E. A. Uehling, Phys. Rev. 48, 55 (1935).
[10]L. W. Fullerton and G. A. Rinker, Jr., Phys. Rev. A 13, 1283 (1976).
[11]C. W. Nestor, private communication; C. C. Lu *et al.*, At. Data 3, 1 (1971).
[12]W. G. Lynch *et al.*, to be published.

Measurement of the g Factor of the ^{237}Pu Short-Lived Fission Isomer

M. H. Rafailovich, E. Dafni,[a] G. Schatz,[b] S. Y. Zhu,[c] K. Dybdal,[d] S. Vajda, C. Alonso-Arias, and G. D. Sprouse
Department of Physics, State University of New York, Stony Brook, New York 11794
(Received 29 December 1981)

The perturbed-angular-distribution method has been used to measure the g factor of the τ=122(10)-nsec fission isomer in ^{237}Pu. To eliminate unwanted perturbations, a special cubic nonparamagnetic alloy, $^{235}UIr_2$, was heated to 950 °C and used as the target. The quantities measured were $A_{22}=+0.21(6)$ and $g=-0.45(3)$. The g factor is consistent with the $I=\frac{5}{2}$ ground state of the 871 $\frac{1}{2}^+$ Nilsson orbital, and the fission anisotropy is consistent with $K=\frac{1}{2}$ at the second saddle point.

PACS numbers: 21.10.Ky, 21.10.Pc, 27.90.+b

The fission isomers offer a unique opportunity to study nuclear structure at large deformations, and several beautiful experiments[1,2] have shown that the isomers have axis ratios of the order of 2 to 1. With the exception of ^{239}Pu,[3] more detailed information on the structure of these interesting nuclei has not yet been obtained because of the difficulty of making magnetic-moment measurements in the actinides. The perturbed-angular-distribution technique usually employed for g-factor measurements of isomeric states requires that the nuclear alignment be preserved

for a time sufficient to observe a precession of the isomer in an applied magnetic field. Although a magnetic-moment measurement of ^{237}Pu($\tau \approx 1$ μsec) was reported,[4] subsequent attempts to perform similar experiments have not been successful,[5] presumably because of loss of the fission anisotropy by various mechanisms. In this Letter we report a measurement of the g factor of the $\tau \approx 0.1$-μsec fission isomer in ^{237}Pu where new techniques have been used to avoid this alignment loss.

Since the actinides have an unfilled $5f$ electron shell, they are in general paramagnetic, and this gives rise to two difficulties. First, the effective field at the nucleus will be the external field plus the time-averaged hyperfine field. The effective field depends on the temperature of the host and on the charge state of the atom in the metallic host. Ancillary experiments which are very time consuming must be performed to determine these parameters. In addition, the atomic spin fluctuations of the actinide atom can relax the nuclear alignment via the hyperfine coupling. Whether or not this occurs depends on the fluctuation time, τ_c, which is not well known for the actinide elements. To circumvent these difficulties, we have chosen a cubic nonparamagnetic alloy of uranium, UIr_2, as the target host in our experiments. The analogous alloy $PuIr_2$ is also cubic and not paramagnetic. These alloys are extremely dense with small atomic spacings, and their magnetic properties are known to be quenched for small actinide-actinide distances.[6] In addition the chemical stability of the alloy greatly facilitated the target production and handling.

The experimental arrangement is shown in Fig. 1. The nuclear reaction ^{235}U$(\alpha, 2n)^{237m}$Pu was effected by a beam of 25.2-MeV α particles from the Stony Brook FN tandem Van de Graaff accelerator. Before injection into the tandem accelerator the beam was swept across an aperture every 2 μsec, producing a pulse approximately 40-nsec wide. This pulse was bunched to about 2 nsec, and another set of plates after the tandem accelerator was used to sweep away any particles not arriving in the pulse. For some experiments, an 0.5-μsec repetition period was used. The dark current between pulses was monitored by a solid-state detector at 45° to the beam direction. Foils were placed in front of this detector to stop all fission fragments so that only Coulomb-scattered α particles were observed. The total dark current between zero crossings of the post-acceleration sweeper was less than 10^{-8} of the prompt intensity, as compared with the delayed to prompt fission intensity of 10^{-5}.

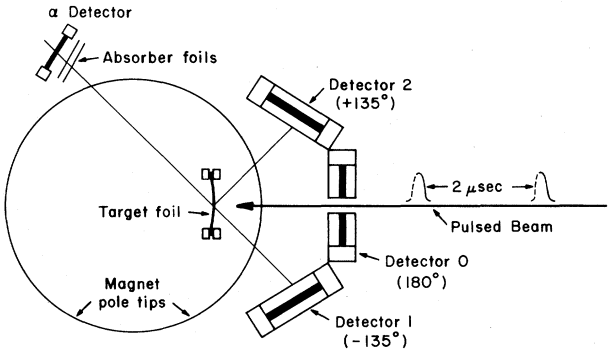

FIG. 1. Experimental arrangement.

The target consisted of 4 mg/cm^2 of $^{235}UIr_2$ sputtered onto a 4 mg/cm^2 molybdenum backing. To continuously anneal any radiation damage present in the target, it was heated to 950 °C by passing a current through the foil. The temperature and resistance of the target were monitored closely. After an initial drop in resistance of several percent associated with annealing of the sputtered alloy, the resistance remained constant for several days for pressures lower than 2×10^{-7} Torr. This pressure was maintained by a cryopump and by a liquid-nitrogen shield surrounding the target. Even a brief pressure excursion, such as from warming the shield, resulted in an increase in the resistance of the target. Subsequent x-ray analysis of a target with increased resistance indicated the presence of uranium oxides. Targets maintained in good vacuum showed predominantly UIr_2 lines and only these data were used for the g-factor measurements. Data from targets which showed oxidation were used only for the lifetime and isomer ratio determination.

The fission fragments were observed by 450-mm^2, 100-μm-thick solid-state detectors (see Fig. 1). Their outputs were fed into fast differential discriminators whose levels were set well above any pulses from α particles. Signals from detectors 1 and 2 were added together and used to start a time-to-amplitude converter which was stopped by a signal from the beam pulsing system. A second set of signals from the discriminators was used to route these time spectra into quadrants of a multichannel analyzer. An identical system was used for detector 0 and the α detector. The electronic systems were checked by introducing random pulses from a pulser while the intense prompt counting rate was present, and a constant delayed spectrum was observed.

From the measured delayed time spectra in detectors 1 and 2, the ratio $R(t) = (N_1 - N_2)/(N_1 + N_2)$ was formed as it is most sensitive to a precessing angular distribution. The ratio functions for two different runs are shown in Figs. 2(a) and 2(b), along with least-squares fits by the function

$$R(t) = \frac{3A_2}{4 + A_2} \sin 2\left(\frac{g\mu_N B}{\hbar} t - \Delta\varphi\right), \quad (1)$$

where A_k is the coefficient of $P_k(\cos\theta)$ in the angular distribution of the fission fragments and $\Delta\varphi$ accounts for a small deflection of the beam.

Although individual points are in general only two standard deviations away from isotropy, the systematic deviations are correlated in time and they reversed sign when the field was reversed. The sign of the anisotropy is determined from the phase of the oscillations in the 180° detector, which are shown in Fig. 2(c). The parameters obtained from the least-squares fits of these data are shown in Table I. The lifetime deduced from the sum of the data was $\tau = 122(10)$ ns. The

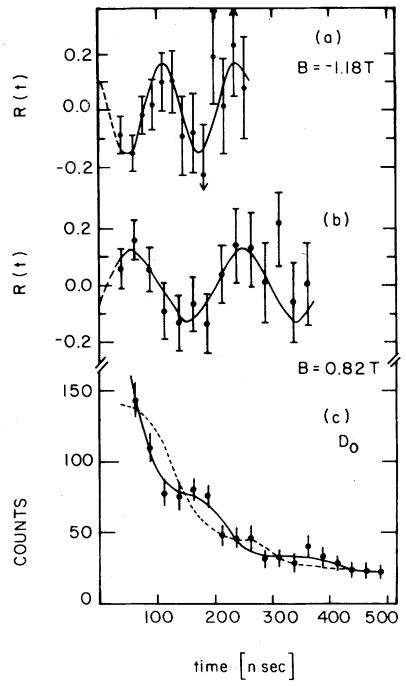

FIG. 2. (a) Ratio function formed from detectors 1 and 2. For this data 0.5-μsec repetition period was used. The smooth curve is a least-squares fit of Eq. (1). (b) Ratio function as in (a) but with 2-μsec pulse repetition period. Note the reversal of the initial phase when the direction of the magnetic field was reversed relative to (a). (c) Time spectrum in the 180° detector taken simultaneously with (b). The solid (dashed) curve corresponds to A_2 positive (negative).

ratios of production cross sections for the isomers were determined as $\sigma_{\text{short}}/\sigma_{\text{long}} = 0.36(6)$, and $\sigma_{\text{short}}/\sigma_{\text{prompt}} = 5.4(3) \times 10^{-6}$. The values $A_2 = +0.21(6)$ and $g = -0.45(3)$ are adopted from the average of all the data in Table I. An upper limit of $A_4 \leq 0.12$ was also determined from these data. The A_k have been corrected for finite solid angle of the detectors. From the temperature-independent susceptibility of the $PuIr_2$ (Ref. 6) the correction to the magnetic field was estimated to be less than 2% and was not made.

The lifetime obtained is in excellent agreement with the previous measurements of Refs. 7 and 8, but disagrees with Ref. 9. The short pulsing repetition period used in Ref. 9 makes the separation of the short and the long lifetimes difficult. The anisotropy obtained in Ref. 9 is also in disagreement in sign and magnitude with the present value, possibly because of the same reason. The measured magnitude of the anisotropy A_2 should be viewed as a lower bound, as it is still possible that some fraction of the nuclei are relaxed by dealignment processes. The anisotropy is consistent with an $I = \frac{3}{2}$ or $\frac{5}{2}$ level fissioning through a state with $K = \frac{1}{2}$ at the second saddle point, although other values of I and K cannot be ruled out from this evidence alone. The measured production ratio of the short- and long-lived isomers is consistent with the previous measurements of Ref. 7 at similar bombarding condition. When coupled with the recent electron-induced fission work,[8] the possible spin of the long-lived isomer is most likely $\frac{9}{2}$ or $\frac{11}{2}$.

The measured g-factor, $-0.45(3)$, is unusually large in magnitude for a deformed odd-N nucleus. The g factor for a deformed nucleus is related to the nuclear quantum numbers by[10]

$$g_K = K^{-1}\langle K | g_l l_3 + g_s s_3 | K\rangle, \quad (2)$$

$$g_I = g_R + (g_K - g_R)[K^2/I(I+1)] \times [1 + b(2I+1)(-1)^{(I+1/2)}], \quad (3)$$

TABLE I. Experimental results.

θ_{detector} (deg)	B (T)	g	A_2 [a]	$\Delta\varphi$ (deg)
±135	−1.18	−0.44(6)	+0.23(10)	15(22)
±135	+0.82	−0.44(4)	+0.20(7)	−2(11)
180 [b]	+0.82	−0.47(5)	+0.22(7)	10(16)

[a] The quoted values have been multiplied by 1.2 to correct for finite solid angle.

[b] The 180° data were fitted by the function $Ne^{-t/\tau}\{1 + [3A_2/(4+A_2)]\cos 2[(g\mu B/\hbar)t - \Delta\varphi]\}$.

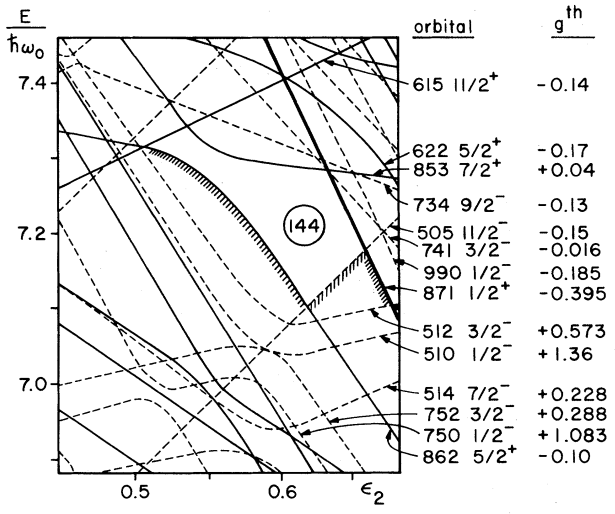

FIG. 3. Nilsson model levels using the modified oscillator parameters from Ref. 11. The g factors which label each state are calculated at $\epsilon_2 = 0.61$ and $\epsilon_4 = 0.065$. For ^{237}Pu($N = 143$), $\hbar\omega_0 = 7.08$ MeV.

where b, the magnetic decoupling factor, is zero except for $K = \frac{1}{2}$ bands. Since the main contribution to the magnetic moment for odd-neutron nuclei is the spin moment of the neutron, states with large g factors must necessarily have small orbital angular momentum since the g factor is the ratio of magnetic moment to angular momentum. From Eq. (3), we also see that intrinsic states with large negative g factors are made more positive by the rotational contribution, g_R. Only if we consider $K = \frac{1}{2}$ bands with the decoupling term in the magnetic moment can we achieve large negative g factors.

Figure 3 shows the states obtained by Moller *et al.*[11] with a modified oscillator potential using the standard Nilsson model parameters, $\mu = 0.325$ and $\kappa = 0.0635$, as a function of ϵ_2 deformation. In this calculation, the second minimum of energy was obtained at $\epsilon_2 = 0.61$, $\epsilon_4 = 0.065$. Leander[12] has calculated the g factors of these states at this deformation with $g_R = 0.4$, $g_l = 0$, and $g_s = 0.7 \times g_s$(free). The only state with large negative g factor within 2 MeV of the Fermi level ($N = 143$ for ^{237}Pu) is the 871 $\frac{1}{2}^+$ state, where the calculated decoupling parameter, $a = -1.75$, puts the $I = \frac{3}{2}$ member of the $K = \frac{1}{2}$ band lowest. The dependence of the g factor and of the level ordering of the $K = \frac{1}{2}$ band on deformation was tested by varying ϵ_2 and ϵ_4 around the minimum energy values. Variation of ϵ_2 from 0.58 to 0.64 or ϵ_4 from 0.055 to 0.075 did not change the level order in the band while the g factor varied from -0.53 to -0.28 or -0.32 to -0.49, respectively. For deformations $\epsilon_2 > 0.64$ or $\epsilon_4 < 0.055$ the ground-state spin changes to $I = \frac{1}{2}$, and no other state with large negative g factor can be found in the calculations.

Several other calculations using different potential shapes or different interaction strengths have been made.[13-15] The 871 $\frac{1}{2}^+$ level appears near the Fermi level in these calculations, but is in general 1 MeV too high in energy. Hamamoto and Ogle[14] have shown that the energy of this level is rather insensitive to the strength of the spin-orbit interaction, and so other higher-order effects[16] may be required to bring the level slightly lower in energy.

Libert, Meyer, and Quentin[17] have utilized a self-consistent Hartree-Fock calculation and obtained states in the second minimum which are very strongly mixed. A state with $I = \frac{3}{2}$, $K = \frac{1}{2}$, and $g = -0.55$ is found for ^{237}Pu, but the calculated decoupling parameter of ≈ -1 does not definitely place the $\frac{3}{2}$ member of the $K = \frac{1}{2}$ band as the ground state. The nature of this strongly mixed state should be studied in more detail to determine whether it offers an alternative explanation of the measured properties of the ^{237}Pu fission isomer.

The measured g factor is very unusual for an odd-N nucleus and can only be explained by a very limited number of configurations. This fact should aid in further attempts to understand nuclear structure at large deformation.

This work was supported in part by the National Science Foundation. We wish to thank Dr. Georg Leander for supplying the Nilsson model calculations and for many helpful discussions. We are indebted to Dr. D. J. Lam for discussions about the magnetic properties of the actinides. The support and help of our colleagues, especially Professor P. Paul, Dr. J. M. Brennan, and Dr. J. Noè throughout this work is gratefully acknowledged. We wish to thank Mr. W. D. Riel, Mr. E. Vapirev, Mr. S. Rolston, and Mr. X. L. Gu for their assistance in the experimental work.

---

[a]Permanent address: Weizmann Institute, Rehovot, Israel.

[b]Permanent address: Konstanz University, Konstanz, Germany.

[c]Permanent address: Atomic Energy Institute, Peking, China.

[d]Permanent address: Aarhus University, Aarhus, Denmark.

[1]V. Metag, D. Habs, and H. J. Specht, Phys. Rep. 65, 1–41 (1980).

[2]C. E. Bemis, J. R. Beene, J. P. Young, and S. D. Kramer, Phys. Rev. Lett. 43, 1854 (1979).

[3]H. Backe, R. Lichter, D. Habs, V. Metag, J. Pedersen, P. Singer, and H. J. Specht, Phys. Rev. Lett. 42, 490 (1979).

[4]R. Kalish, B. Herskind, J. Pedersen, D. Shackleton, and L. Strabo, Phys. Rev. Lett. 32, 1009 (1974).

[5]D. Habs, S. Hanna, B. Herskind, V. Metag, P. Paul, J. Pedersen, G. Schatz, G. Sletten, and H. J. Specht, Max-Planck Institut fur Kernphysik, Heidelberg, Annual Reports 1975, 1976, and 1977 (unpublished).

[6]D. J. Lam and A. T. Aldred, in *The Actinides—Electronic Structure and Related Properties*, edited by A. J. Freeman and J. B. Darby (Academic, New York, 1974), Vol. I.

[7]P. A. Russo, R. Vandenbosch, M. Mehta, J. R. Tesmer, and K. L. Wolf, Phys. Rev. C 3, 1595 (1971).

[8]W. Gunther, K. Huber, U. Kneissl, H. Krieger, and H. J. Maier, Phys. Rev. C 19, 433 (1979).

[9]H. J. Specht, E. Konecny, J. Weber, and C. Kozhuharov, in *Proceedings of the Third Symposium on the Physics and Chemistry of Fission, Rochester, New York, 1973* (International Atomic Energy Agency, Vienna, Austria, 1974), Vol. I, p. 285.

[10]A. Bohr and B. Mottleson, *Nuclear Structure* (Benjamin, New York, 1975), Vol. II.

[11]P. Moller, Nucl. Phys. A192, 529 (1972).

[12]G. Leander, private communication.

[13]P. Moller and J. R. Nix, in *Proceedings of the Third Symposium on the Physics and Chemistry of Fission, Rochester, New York, 1973* (International Atomic Energy Agency, Vienna, Austria, 1974), Vol. I, p. 103.

[14]I. Hamamoto and W. Ogle, Nucl. Phys. A240, 54 (1975).

[15]H. C. Pauli, Phys. Rep. 7C, 35 (1973).

[16]S. G. Nilsson, F. Tsang, A. Sobiezewski, Z. Szymanski, S. Wycech, C. Gustafson, I. L. Lamm, P. Moller, and B. Nilsson, Nucl. Phys. A131, 1 (1969).

[17]J. Libert, M. Meyer, and P. Quentin, Phys. Lett. 95B, 175 (1980).

Isospin Splitting of the Giant Dipole Resonance in ^{60}Ni

T. J. Bowles,[a] R. J. Holt, H. E. Jackson, R. D. McKeown,[b] A. M. Nathan, and J. R. Specht

Physics Division, Argonne National Laboratory, Argonne, Illinois 60439, and University of Illinois at Urbana-Champaign, Urbana, Illinois 61801

(Received 15 July 1981)

The most stringent test to date of the concept of isospin splitting of the giant dipole resonance in a medium-weight nucleus has been performed by a study of the (γ, n_0), (γ, p_0), and (γ, γ) reaction channels for ^{60}Ni. The ground-state photoneutron cross section for ^{60}Ni was measured and compared with the already known (γ, p_0) reaction cross section in order to demonstrate isospin splitting. The relative strength and separation of the isospin-dependent components of the resonance were estimated from an analysis of photon scattering data.

PACS numbers: 25.20.+y, 24.30.Cz, 27.50.+e

It is widely accepted that in nuclei with a neutron excess [$T \equiv (N-Z)/2 > 0$], the isovector giant dipole resonance (GDR) is shared between a $T_< \equiv T$ and a $T_> \equiv T+1$ component and that these components are split in energy, primarily by the nuclear symmetry potential.[1,2] Fallieros and collaborators have developed an extended schematic model, which we refer to as the isospin splitting model (ISM), in which the $T_<$ and $T_>$ dipole states are predicted to be separated by an amount[1]

$$\Delta E = 60(T+1)/A \text{ MeV}, \quad (1)$$

and to have dipole matrix elements in the ratio[2]

$$R = \frac{|r_>|^2}{|r_<|^2} = \frac{1}{T}\,\frac{1-1.5TA^{-2/3}+T(T-\frac{1}{2})/NZ}{1+1.5A^{-2/3}-(T-\frac{1}{2})/NZ}, \quad (2)$$

where $A = N+Z$. Although both these predictions are fairly well supported by data on light nuclei,[3] previous experiments on medium-weight nuclei have concentrated primarily on the energy splitting.[4] There has not yet been a quantitative test of Eq. (2) in a medium-weight nucleus. In this Letter we reinvestigate the question of isospin splitting in ^{60}Ni. We will show that a new measurement of the ^{60}Ni(γ, n_0) cross section and a reanalysis of the ^{60}Ni(γ, γ) data provide confirming evidence for the predictions of the ISM.

Diener *et al.*[5] already have considered the question of isospin splitting in ^{60}Ni and have measured the ^{59}Co$(p, \gamma_0)^{60}$Ni cross section throughout the giant-resonance region. These data [see Fig. 1(a)] indicate two peaks located near 17 and 20 MeV. At that time, the total (γ, n) data of

